

Designing Ethereum’s Geographical (De)Centralization Beyond the Atlantic

Sen Yang^{1,2,3}, Burak Öz^{3,4}, Fei Wu⁵, and Fan Zhang^{1,2}

¹ Yale University

² IC3

³ Flashbots

⁴ Technical University of Munich

⁵ King’s College London

Abstract. Decentralization has a geographic dimension that conventional metrics such as stake distribution overlook. Where validators run affects resilience to regional shocks (outages, disasters, government intervention) and fairness in reward access. Yet in permissionless systems, locations cannot be mandated, but they emerge from incentives. Today, Ethereum’s validators cluster along the Atlantic (EU and U.S. East Coast), where latency is structurally favorable. This raises a key question: when some regions already enjoy latency advantages, how does protocol design shape validator incentives and the geography of (de)centralization? We develop a latency-calibrated agent-based model and compare two Ethereum block-building paradigms: a Single-Source Paradigm (SSP), akin to MEV-Boost, where proposers fetch full blocks from a relay that also propagates them; and a Multi-Source Paradigm (MSP), where proposers aggregate value from multiple sources and broadcast the block themselves. Simulations show that SSP concentrates around relay placement but more slowly, since proximity mainly affects propagation, and the marginal value of time is relatively uniform across regions. MSP centralizes faster: aggregating across sources makes marginal value location-dependent, amplifying payoff dispersion and migration toward latency minima. Source placement and consensus settings can dampen or intensify these effects, though once validators are already clustered, the impact of source placement on decentralization is marginal. In most cases, North America consistently emerges as the focal hub. These findings show that protocol design materially shapes validator geography and offer levers for promoting geographical decentralization.

Keywords: Geographical decentralization · Ethereum · Simulation

Acknowledgments

The authors appreciate Quintus Kilbourn, Lioba Heimbach, Thomas Thiery, Devan Mitchem, Akaki Mamageishvili, István András Seres, Bruno Mazonra, and Christoph Schlegel for helpful discussions and comments. Fei Wu acknowledges support from a Flashbots research grant.

1 Introduction

Decentralization is the core security assumption of permissionless blockchains, shaping properties such as integrity, safety, availability, and censorship resistance [33,18,44,50]. These critical security properties typically rely on assumptions that at least a certain fraction of participants in a system follow the rules or that conflicting incentives prevent collusive behaviour, i.e., that participant behaviour is not centrally controlled or highly correlated. Measuring decentralization requires more than ascertaining who controls mining power or stake; the geographic distribution of participants also matters.

Geographical decentralization is particularly important for two reasons. First, security assumptions depend on participants not being overly correlated. If a large share of validators are co-located, they become jointly vulnerable to external shocks such as natural disasters or power outages, as well as jurisdictional risks such as government intervention. A clear example is the 2021 ban on Bitcoin mining in China, which triggered a sharp and sudden drop in global hash rate and forced miners to relocate at scale [43]. Second, geography affects fairness: validators in remote regions may face structural disadvantages in capturing rewards. Yet achieving geographical decentralization is non-trivial, since in permissionless blockchains, participant geo-locations cannot be mandated by protocol but instead emerge endogenously from its incentive structure.

Today, despite Ethereum’s large validator set, existing data [8] reveal heavy concentration along the Atlantic, particularly in Europe (EU) and the U.S. East Coast of North America (NA) (see Figure 1a). This concentration raises a question: why do validators cluster around the Atlantic rather than distribute more evenly across the globe? This pattern resembles classical models of spatial competition, such as Hotelling’s law [25], where agents tend to cluster when relative advantages exist. Similarly, although Ethereum validators are not directly competing for physical location, latency advantages can create analogous incentives to concentrate geographically. As shown in Figure 1b, regions with advanced network infrastructure—particularly EU and NA—consistently offer lower latencies to other regions.

As a result, validators in these regions gain a structural advantage. Lower latency improves their ability to (i) attest correctly and collect consensus reward, and (ii) propose blocks successfully by collecting enough attestation in time. These advantages also extend to timing games [36,39], where validators strategically delay block release for more revenue. In combination, such latency benefits create strong incentives for validators to cluster geographically, reinforcing centralization pressures despite the protocol’s decentralized design.

These observations raise a pressing research problem: *given persistent regional advantages, how do protocol rules shape validator incentives and the resulting dynamics of Ethereum’s geographical (de)centralization?* While latency is an important factor, it is not the only structural force at play. In particular, protocol design choices—most notably the block-building and consensus pipeline—can either amplify or mitigate centralization pressures. For instance, today’s Proposer-Builder Separation (PBS) implementation, MEV-Boost [14],

channels value through relays that function simultaneously as exclusive providers of builder bids and as block propagators, making them natural focal points for proposers. By contrast, when validators construct blocks locally, value originates from multiple sources (e.g., mempools) and block propagation is handled directly by the proposer. Understanding these dynamics is essential for assessing how today’s protocol design affects validator incentives and the resulting pressures toward or against geographical decentralization.

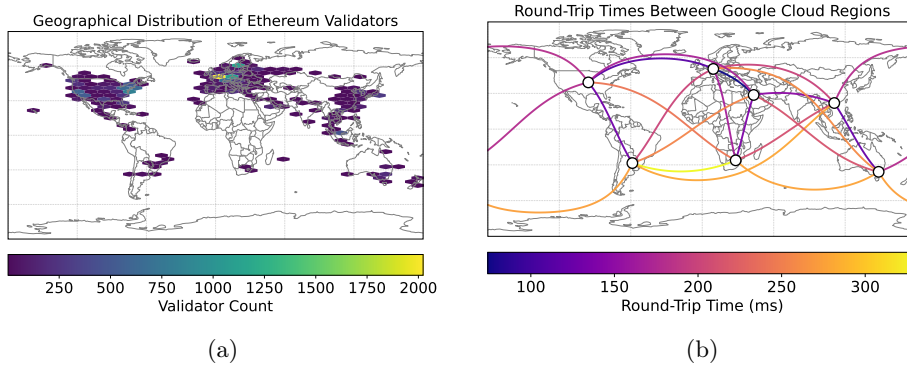


Fig. 1: Validator distribution (a) and inter-region Internet latencies (b) highlight the structural forces behind Ethereum’s geographical centralization. Validator location data covers $\sim 16,000$ Ethereum validators, provided by Chainbound [8]. Latency values are macro-regional medians of round-trip times between Google Cloud regions (see Section A).

Empirical and theoretical limitations. Many existing studies focus on mining power or stake distribution [10,20,4], and even when empirical measurements capture validator geography [7,13,26], they remain limited: they describe the current distribution but cannot predict counterfactuals or future protocol effects. Moreover, measurements conflate multiple factors—infrastructure, protocol-level components (e.g., MEV-Boost [14] and its relays), and heterogeneous validator strategies—making causal attributions unclear. Purely theoretical analyses fare no better: the interplay of heterogeneous strategies, network latencies, and protocol rules generates a state space too complex for tractable modeling.

Addressing the gaps with simulation. To overcome these limitations, we develop an agent-based simulation framework that isolates and quantifies the effects of validator geography. Agent-Based Modeling (ABM) [31] is well-suited for this setting because it accommodates heterogeneous validator behaviors and their interactions with infrastructure and protocol components. Unlike empirical measurements, our framework supports counterfactual analysis and controlled variation of these factors, providing a comprehensive view of how geographic concentration shapes Ethereum’s decentralization and liveness.

Table 1: Effects of block-building paradigms (SSP, MSP), validator distribution, and source placement on geographical (de)centralization.

| Distribution* | Effects [§] |
|---------------|-----------------------------------------------------------------------------------------------------------------------------------------------------------------------------------------------------------------------------------------------------------------------|
| ○, ○ | In SSP, proximity affects only propagation, so value accrual is uniform and centralization occurs slowly around relays. In MSP, value aggregates across regions, making accrual location-dependent, amplifying payoff heterogeneity, and accelerating centralization. |
| ○, △ | Placing information sources in low-latency regions dampens validator centralization in SSP but strengthens it in MSP, whereas high-latency placement has the opposite effect. |
| △, ○ / △, △ | With Ethereum’s already centralized validator distribution, SSP may temporarily incentivize validators to co-locate with relays outside incumbent hubs, whereas in MSP source placement has minimal impact once clustering is established. |

* Distribution refers to the geography of validators and information sources. The first entry denotes validators, the second information sources. ○ = homogeneous, △ = heterogeneous.

§ Consensus parameters further impact these dynamics. Across nearly all settings, North America consistently emerges as the latency minimum and the centralization focal point.

To the best of our knowledge, this is the first study to investigate the geographical decentralization of Ethereum validators through simulation. We make the following contributions:

- We propose and implement a simulation framework that models validator interactions under the consensus protocol, enabling controlled experimentation under different geographic and protocol configurations.
- Using a model calibrated with real-world latency data, we analyze validator strategies under two block-building paradigms—the Multi-Source Paradigm (MSP) and the Single-Source Paradigm (SSP)—to assess how protocol design influences validator incentives in geographical positioning.
- Our latency-calibrated simulations indicate that protocol design plays a major role in validator centralization. Table 1 summarizes these effects together with validator and information source placement.
- We provide a public dashboard of our simulation results [3], along with the simulation framework itself [51], to support future research on geographical decentralization.

2 Background

Proof-of-Stake Ethereum. Ethereum has operated under Proof-of-Stake (PoS) since September 2022 [17]. In PoS, any participant can become a validator by depositing at least 32 ETH as collateral, which aligns incentives with the network’s security [6]. Block production under PoS follows the proposer–attester model. In each 12-second slot, a validator is pseudorandomly selected as the *proposer* to create and broadcast a new block. A committee of validators, also pseudorandomly selected from the active validator set, serves as *attesters* by making attestations on the proposed block. The block is considered valid only if it receives the required number of attestations, as mandated by the protocol.

Maximal Extractable Value. Maximal Extractable Value (MEV) refers to the value that privileged entities (e.g., proposers) can capture by inserting, excluding, or reordering transactions within a block [11]. MEV poses a threat to decentralization by skewing the reward distribution, which in principle should be homogeneous across validators given equal stake. Since effective extraction requires substantial capital, specialized infrastructure, and sophisticated algorithms, MEV can foster centralization by concentrating rewards among well-resourced actors [15].

Proposer-Builder Separation and MEV-Boost. PBS is introduced to enable validators to benefit from MEV rewards, regardless of their resources or infrastructure, by outsourcing block construction (and MEV extraction) to a class of specialized entities called *builders*, thereby reducing the centralization pressure among consensus participants. The current implementation of PBS is MEV-Boost [14], where the proposer conducts an auction among builders through a trusted third party (*relay*) to obtain the most valuable block. Under PBS, the MEV of a transaction typically refers to the priority fee plus direct transfer to the builder from order flow providers (e.g., searchers) alongside their transaction [37,46]. A proposer may strategically delay block publishing to gain additional MEV from transactions arriving later. This behavior is known as timing games [36,39].

Agent-Based Modeling. ABM studies complex systems by specifying individual entities (*agents*) and the rules governing their behaviors [31]. It is particularly suited to settings with heterogeneous participants, adaptive decision-making, and interactions that resist closed-form analysis. An ABM typically consists of agents situated in an *environment*, each following a set of *strategies*. The environment provides context and constraints, while agents respond based on their strategies. By modeling and simulating local interactions, ABM reveals how individual incentives generate emergent system-level outcomes.

3 Simulation Framework

In this section, we present our agent-based simulation framework together with the metrics designed to measure geographical decentralization.

Specifically, we study the implications of two block-building paradigms for Ethereum’s decentralization, which differ in how a block is built and distributed: (i) the *Multi-Source Paradigm* (MSP), where a validator aggregates information distributed across regions to build the block and propagate the block, and (ii) the *Single-Source Paradigm* (SSP), in which a validator outsources block building and propagation to a single third-party.

These paradigms mirror current practice: MSP corresponds to validators self-building blocks without MEV-Boost by gathering order flow from diverse sources, while SSP corresponds to relay-mediated block procurement under MEV-Boost.

3.1 Model

Our model builds on ABM techniques and captures the heterogeneous validator strategies and their interactions under the consensus protocol. The system consists of autonomous agents whose incentive-driven behaviors collectively generate global outcomes. The canonical components of the model are as follows.

Geographical regions and latency. We model geography as a finite set of discrete regions $\mathcal{R} = \{r_1, r_2, \dots, r_m\}$. For any two regions $r_j, r_k \in \mathcal{R}$, define the random propagation latency of a message $d(r_j, r_k)$. We assume $d(r_j, r_k)$ is drawn from a log-normal distribution with parameters known to agents $\ln[d(r_j, r_k)] \sim \mathcal{N}(\mu_{jk}, \sigma^2)$, and the expected latency can be given by $\mathbb{E}[d(r_j, r_k)] = e^{\mu_{jk} + \sigma^2/2}$. This abstraction simplifies geographical modeling and reflects reality, as inter-region latencies do not necessarily increase with geographical distance.

Agents. Each validator in the set $\mathcal{V} = \{v_1, \dots, v_P\}$ is modeled as an autonomous agent. An agent v_i is characterized by the following attributes:

- *Stake* $s_i \in \mathbb{R}_{\geq 0}$, which determines both the probability of proposer selection and attestation weight. For tractability, we assume that all validators hold equal and constant stakes.
- *Region* $r_i \in \mathcal{R}$, which determines the latency for messages exchanged with other agents.

Environment. The environment consists of two components: (i) the consensus protocol, which governs time, proposer selection, and attestation; and (ii) information sources, which determine the value of blocks proposed by the validators. We describe each in turn.

Time and consensus. Drawing from the timing games model in [39], we partition time into slots $n \in \{1, \dots, N\}$ of fixed duration $\Delta > 0$. In each slot n , a validator is selected as the proposer p_n , and a set of attesters $\mathcal{A}_n \subseteq \mathcal{V} \setminus \{p_n\}$ is assigned to vote on the proposal. A block becomes canonical if at least a fraction $\gamma \in (0, 1]$ of attesters in \mathcal{A}_n vote positively before a cutoff time $\tau_{\text{cut}} \in [0, \Delta]$. The timeliness of attester votes depends on both the block’s release time and the propagation latencies. Attestation success under MSP and SSP is modeled accordingly below. We abstract away the details of fork-choice rules.

Information sources. We define an information source $I \in \mathcal{I}$ as an exogenous generator of the block value, i.e., the aggregate MEV from transactions included in the block. Each source is associated with a region $r(I) \in \mathcal{R}$. In this paper, information sources are assumed to be fungible, with identical value parameters; we vary only their positioning to study homogeneity or heterogeneity effects.

We distinguish two types of sources: $\mathcal{I}_{\text{signal}} \subseteq \mathcal{I}$ and $\mathcal{I}_{\text{relay}} \subseteq \mathcal{I}$. A *signal source* in MSP, contributes only partially to block value—for example, a centralized exchange providing price information which can be arbitrated in on-chain venues. A *relay source* in SSP, by contrast, solely determines the value of the proposed block, as in MEV-Boost relays that deliver builder-constructed blocks directly to proposers. Formally, let $V_I(t)$ denote the value available from source I at elapsed time t within a slot, capturing the dynamic evolution of

extractable value [36,39,45]. For tractability, we model $V_I(t)$ as a deterministic linear function $V_I(t) = a_I t + b_I$, where $a_I > 0$ is the growth rate of extractable value⁶ and $b_I > 0$ is the initial value at the start of the slot, representing pending transactions accumulated since the previous block.⁷

Strategy. We focus on two strategic choices available to a proposer in a slot:

- *Timing:* The proposer chooses a block release time $\tau \in [0, \tau_{\text{cut}}]$, which affects both attestation success and utility.
- *Migration:* Proposers may migrate between regions at cost c . We model migration as instantaneous, justified by pre-synchronization of validator nodes across multiple regions.

MSP Setup

In MSP, block value is derived by aggregating signals from multiple information sources distributed across regions. A proposer’s payoff depends on (i) the latencies to these information sources, which determine how much value can be incorporated, and (ii) the latencies to attesters, which determine whether the block is voted canonical once released.

If proposer p_n in region $r(p_n)$ releases at time τ , it collects value from each signal source $I \in \mathcal{I}_{\text{signal}}$:

$$V_I(\tau - d(r(p_n), r(I))),$$

i.e., the value at an earlier time $\tau - d(r(p_n), r(I))$, offset by the network latency. We assume that values from different signal sources are additive, i.e, the sources do not generate overlapping transactions. Generalizing for an arbitrary region $r \in R$, the aggregate block value observed by a proposer in region r is

$$V_r(\tau) = \sum_{I \in \mathcal{I}_{\text{signal}}} V_I(\tau - d(r, r(I))).$$

Attestation success. After release, each attester $a \in \mathcal{A}_n$ in region $r(a)$ receives the block after a latency $d(r, r(a))$ drawn from log-normal with CDF $F_{d(r, r(a))}$. Attester a votes on time if $\tau + d(r, r(a)) \leq \tau_{\text{cut}}$, which occurs with probability

$$q_a(\tau; r) = F_{d(r, r(a))}(\tau_{\text{cut}} - \tau) \mathbf{1}\{\tau < \tau_{\text{cut}}\}.$$

Let

$$S(\tau; r) = \sum_{a \in \mathcal{A}_n} \text{Bernoulli}(q_a(\tau; r))$$

⁶ In practice, order flow may evolve non-linearly. For example, arbitrage opportunities may surge just before block proposal, following external price signals.

⁷ The initial value b_I corresponds to the reward a proposer would earn if it released immediately, i.e., without delaying to play timing games.

denote the number of timely attestations. Then $S(\tau; r)$ follows a Poisson–binomial distribution, and the probability that the block becomes canonical is

$$\Pi_r(\tau) = \Pr[S(\tau; r) \geq \lceil \gamma |\mathcal{A}_n| \rceil].$$

Optimal release time. A proposer in region r aims to release as late as possible to maximize $V_r(\tau)$, subject to ensuring sufficiently high canonicalization probability. Since $V_r(\tau)$ is modeled as deterministic and the latency distribution is known, at the slot start, the builder solves the optimal release time

$$\tau_r^* = \max\{\tau \in [0, \tau_{\text{cut}}] : \Pi_r(\tau) \geq R\},$$

where R represents the proposer’s risk tolerance, capturing its willingness to engage in timing games at the cost of a higher probability that the block fails to reach some attesters. The corresponding expected payoff is

$$W(r) = \Pi_r(\tau_r^*) V_r(\tau_r^*).$$

Remark 1. For a large committee $|\mathcal{A}_n|$, the randomness of $S(\tau; r)$ concentrates around its mean. By the Law of Large Numbers with $\zeta_r(\tau) = \frac{1}{|\mathcal{A}_n|} \sum_a q_a(\tau; r)$, we have $\Pi_r(\tau) \approx \mathbf{1}\{\zeta_r(\tau) \geq \gamma\}$. In this approximation, τ_r^* is essentially the critical time where $\zeta_r(\tau)$ drops below γ .

Migration decision. At the slot start, the proposer compares $W(r)$ across all regions $r \in R$. As migration incurs a cost c , the proposer moves from its current location $r(p_n)$ only if the *marginal benefit* of migration exceeds the cost

$$\max_{r \in R \setminus \{r(p_n)\}} W(r) - W(r(p_n)) > c,$$

in which case, it re-locates to

$$r^* = \arg \max_{r \in R \setminus \{r(p_n)\}} W(r),$$

and releases the block at $\tau_{r^*}^*$. Otherwise, it stays in $r(p_n)$ and releases at $\tau_{r(p_n)}^*$. This captures the strategic decisions of proposers to maximize expected payoff by jointly optimizing release timing and region choice.

SSP Setup

Relative to the MSP setup, two aspects change: (i) block value is determined by relay bids rather than direct aggregation of signal sources, and (ii) block propagation originates from the selected relay’s region rather than the proposer’s.

If the proposer in region $r(p_n)$ considers relay $I \in \mathcal{I}_{\text{relay}}$ located in $r(I)$, it observes the relay’s bid with latency $d(r(p_n), r(I))$. At release time τ , relay I ’s effective bid value is

$$V_I(\tau) = V_I(\tau - d(r(p_n), r(I))).$$

Attestation success. Once selected by the proposer, relay I broadcasts the block to attestors. Compared to the no-relay case, an additional latency $d(r(p_n), r(I))$ is incurred for the proposer-relay connection, so the timely-attestation probability is now relay-specific:

$$q_a(\tau; I) = F_{d(r(p_n), r(I)) + d(r(I), r(a))}(\tau_{\text{cut}} - \tau) \mathbf{1}\{\tau < \tau_{\text{cut}}\}.$$

The canonicalization probability is thus

$$\Pi_I(\tau) = \Pr \left[S(\tau; I) \geq \lceil \gamma |A_n| \rceil \right].$$

Optimal release time. For each relay I , the release time and associated utility are:

$$\tau_I^* = \max\{\tau \in [0, \tau_{\text{cut}}] : \Pi_I(\tau) \geq R\}, \quad W(I) = \Pi_I(\tau_I^*) V_I(\tau_I^*).$$

Co-location decision. At the slot start, the proposer compares the best relay overall to the best relay accessible without changing location. Let $W^{\text{stay}} = \max_{I \in \mathcal{I}_{\text{relay}}(r(p_n))} W(I)$ be the best relay utility without moving. The proposer migrates iff

$$\max_{I \in \mathcal{I}_{\text{relay}}} W(I) - W^{\text{stay}} > c,$$

in which case it relocates to the region of a relay $I^* \in \arg \max_{I \in \mathcal{I}_{\text{relay}}} W(I)$ and releases at $\tau_{I^*}^*$; otherwise it stays in $r(p_n)$ and uses the best local relay.

3.2 Evaluation Metrics

We next introduce metrics that quantify geographical centralization in our simulations; formal definitions appear in Section C. To characterize how stake is distributed across geographical units (countries/regions; hereafter “regions”), we use the Gini coefficient (inequality, denoted Gini_g) and the Herfindahl–Hirschman Index (concentration, denoted HHI_g). To capture variation in proposer incentives across regions, we define the geographical payoff coefficient of variation, CV_g , which measures disparities in the best proposer payoffs across regions within a slot. Finally, to quantify how geography impacts consensus liveness, we define the geographical liveness coefficient, LC_g , which reflects the minimum number of regions whose failure can break Ethereum’s liveness. Together, these metrics capture stake inequality and concentration, incentive disparities, and resilience to correlated regional failures.

4 Simulation Experiments

In this section, we use our simulation framework to study how protocol design—specifically, the block-building pipeline under MSP and SSP—shapes the geographical (de)centralization of Ethereum validators. We evaluate this across different initial validator distributions and information source placements, and organize the experiments around four research questions:

- **RQ1 (Paradigm effect):** Holding network and economic parameters fixed, how do MSP and SSP differ in the speed and degree of centralization, and what mechanisms drive these differences?
- **RQ2 (Convergence and locus):** Do validators converge to a concentrated equilibrium? If so, which regions emerge as focal hubs, and why?
- **RQ3 (Source placement):** How does the placement of information sources—aligned with low-latency hubs versus misaligned into high-latency regions—amplify or mitigate centralization pressures under each paradigm?
- **RQ4 (Validator distribution):** How does protocol design interact with Ethereum’s current validator geography, which is already skewed toward Europe and North America?

4.1 Simulation Setup

We next specify the setup of our simulation framework.

- **Discrete time:** Time is modeled in discrete steps, with each step corresponding to 50ms to approximate the continuous flow of real time.
- **Simultaneity:** The validators act simultaneously at each time step. For example, once the proposer releases a block, attestors in the same region can immediately attest to it.
- **Regions:** We calibrated the set of regions \mathcal{R} using data from Google Cloud Platform (GCP), which covers 40 regions worldwide. These GCP regions can be further aggregated into seven macro-regions, as detailed in Section A.
- **Latency:** We calibrated the log-normal distribution μ such that expected latency equals the empirical mean latency measured between the corresponding regions on Google Cloud [19]. These measurements are based on two-way delays reported by Google Cloud’s public inter-region latency data, ensuring that our simulation reflects realistic wide-area network conditions. We set $\sigma = 0.5$, but the result can be analogous with other values.
- **Consensus:** We follow the standard Ethereum consensus parameters [16] by setting $\Delta = 12\text{s}$, $\tau_{\text{cut}} = 4\text{s}$, and $\gamma = 2/3$, and assume that all proposers aim to ensure their block becomes canonical with $R = 99\%$. Finally, in all cases, we set $|\mathcal{V}| = 1,000$ validators and $N = 10,000$ slots.
- **Cost:** We first run a baseline with $c = 0$ and, for each of the first 1,000 slots,⁸ record the marginal benefit after migrating to the best region (or relay) for the proposer. The distributions of marginal benefit in both paradigms are shown in Figure 8. Following the Pareto principle, we set $c = 0.002$, as this value would prevent approximately 80% of moves in the baseline simulation with SSP. We present results for other cost settings in Section E.1.

Implementation. We implement our simulation framework [51] using Mesa, a Python-based ABM framework [24]. The framework consists of about 4.6K lines

⁸ We focus on the first 1,000 slots to capture pre-steady-state incentives: with $c = 0$ validators quickly relocate toward high-payoff regions, after which marginal benefit collapse toward zero; using an early window avoids this collapse.

of code. We conducted experiments on a testbed with Intel Xeon Platinum 8380 (80 cores), 128GB RAM, running 64-bit Ubuntu 22.04 as the operating system.

4.2 Baseline Dynamics

We first isolate protocol effects by distributing validators and information sources evenly across macro-regions, and then uniformly within each macro-region’s GCP regions. This avoids bias from the uneven global spread of GCP regions,⁹ ensuring parity in both validator density and aggregate information value across macro-regions.¹⁰ We take this setup as a neutral baseline for studying how protocol design alone shapes validator incentives over today’s Internet infrastructure.

Figure 2 presents the evolution of the metrics in the baseline ($c = 0$) and with migration costs ($c = 0.002$). We make four observations. First, across all settings, the Gini and HHI indices increase while the liveness coefficient declines, indicating growing *centralization* even from a uniform initial distribution; the speed and eventual level depend on both the protocol and the migration cost. Second, in the zero-cost case, concentration rises steeply and then plateaus at a high level, since even marginal utility gains trigger relocation. Third, SSP proves more sensitive to migration costs: with $c = 0.002$, concentration progresses slowly and both indices remain low, whereas in MSP, validators continue to migrate and centralization persists, though the eventual level is somewhat lower as suggested by the HHI. Finally, the payoff coefficient of variation (CV_g) starts higher and converges higher under MSP than SSP, indicating greater cross-region reward asymmetry and stronger co-location incentives in MSP.

Takeaway 1. Differences in centralization speed and degree stem from how value accrues. In SSP, proximity matters only for block propagation, so the marginal value of delaying release is essentially uniform across regions. In MSP, block value is an aggregate function of signals from multiple regions, making the marginal value of time location-dependent. This heterogeneity amplifies cross-region payoff variance, strengthens migration incentives, and ultimately increases centralization pressure under MSP.

4.3 Validator Clustering Patterns

Figure 3 shows how validators redistribute across macro-regions over time in the baseline simulation of Section 4.2. This highlights not only the overall degree of centralization but also *where* validators converge, providing a clear signal of which regions enjoy structural advantages.

When migration is free ($c = 0$), validators rapidly converge to North America in both paradigms. This outcome is driven by latency advantages: on average, North America offers the lowest round-trip latency both to attesters and to

⁹ GCP regions are heavily concentrated in Europe, North America, and Asia (see Section A).

¹⁰ Signal sources (MSP) and relays (SSP) are parameterized so that the total signal value matches the relay baseline. Relay parameters: $(a_I, b_I) = (0.4, 0.04)$.

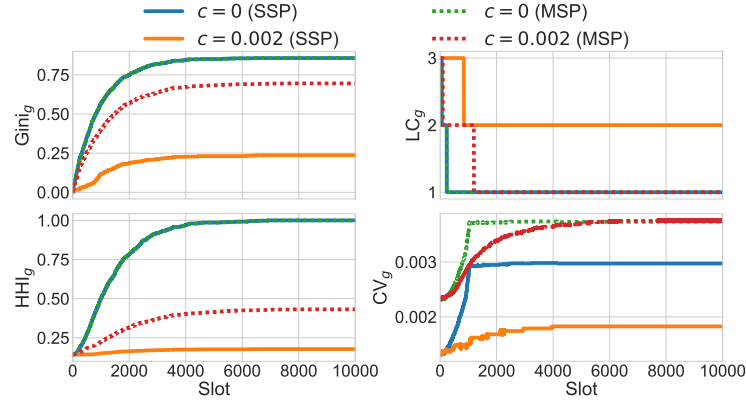


Fig. 2: *Setup: Homogeneous validators and information sources.* Evolution of centralization metrics under SSP and MSP with varying costs $c \in \{0, 0.002\}$.

information sources (see Section A). In the SSP setup, this reduces relay-attester propagation time, giving an edge in timing games. In the MSP setup, the same advantage applies, while proximity to multiple sources further increases expected payoff.

With a migration cost ($c = 0.002$), the patterns diverge. In SSP with homogeneous relays (upper-right panel), migration yields only modest gains: except for validators starting in South America—who benefit from relocating to the Middle East—most regions face weak incentives to move, and the initial distribution persists. In contrast, under MSP (lower-right panel), migration remains advantageous despite costs, and validators continue to concentrate in North America.

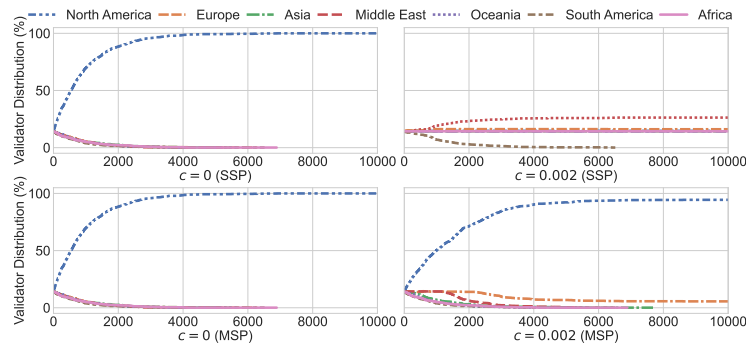


Fig. 3: *Setup: Homogeneous validators and information sources.* Validator distribution aggregated by macro-regions under SSP and MSP with $c \in \{0, 0.002\}$. Early termination of a line means no validators remain in that macro-region.

Takeaway 2. Location of centralization is driven by latency minima: North America emerges as the focal region in both paradigms when migration is free; with costs, MSP still pulls validators toward North America, whereas SSP largely preserves the status quo, apart from South America’s shift toward the Middle East.

4.4 Influence of Information Sources

We next assess how heterogeneous information source placement affects validator incentives under an otherwise neutral validator distribution. Specifically, we test whether (i) placing sources in low-latency macro-regions (e.g., Europe) accelerates centralization, and (ii) placing sources in high-latency macro-regions (e.g., South America) dampens it. In this setting, validators remain evenly distributed across macro-regions (and uniformly within each macro-region’s GCP regions), but source locations are no longer homogenized. We consider two cases: *Latency-aligned*: three information sources placed in `asia-northeast1`, `eu-west1`, and `us-east4` (low average latency); and *Latency-misaligned*: three information sources placed in `africa-south1`, `australia-southeast1`, and `southamerica-east1` (high average latency).¹¹

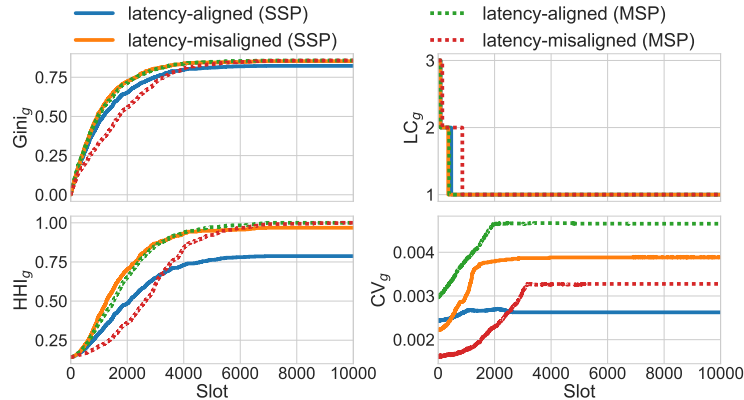


Fig. 4: *Setup: Homogeneous validators with heterogeneous information sources.* Evolution of centralization metrics under SSP and MSP with latency-aligned vs. latency-misaligned source placement ($c = 0.002$).

With a migration cost of $c = 0.002$, Figure 4 yields two observations. First, under SSP, centralization progresses more slowly in the latency-aligned case than in the latency-misaligned case. The intuition is that, when relays already

¹¹ Relay value parameters match the previous setting; signal sources are calibrated to the same baseline.

sit in well-connected hubs, the proposer–relay round trip is small even without moving; co-location only marginally improves bid recency, which often fails to justify the migration cost. By contrast, when relays are placed in poorly connected regions, non-colocated proposers face large proposer–relay latencies, making co-location yield a bigger utility jump that more often justifies paying c . Thus, with costs, placing relays in globally well-connected regions reduces the marginal benefit of co-location and promotes more symmetric access to value.

Second, under MSP, we observe the opposite pattern: the latency-aligned case centralizes faster than the latency-misaligned case. Because proposers both aggregate value from sources and broadcast the block, they must balance proximity to attesters against proximity to sources. When these coincide (latency-aligned placement), moving to a low-latency hub simultaneously improves signal sourcing and propagation, so the marginal utility of migration more often exceeds the cost. By contrast, with latency-misaligned placement (e.g., sources in Africa or South America), improving proximity to sources typically worsens proximity to many attesters, sharpening the trade-off and slowing centralization.

Takeaway 3. Heterogeneous source placement has opposite decentralization effects across paradigms. In SSP, latency-aligned sources (in well-connected hubs) reduce the marginal benefit of migration by making value more symmetrically accessible, thereby encouraging geographical decentralization. In MSP, latency-misaligned sources dampen centralization by forcing proposers to trade off latency to attesters versus latency to signals, which weakens the incentive to concentrate in a single hub.

4.5 Real-World Validator Distribution

We now examine how protocol design interacts with Ethereum’s existing validator geography. Validators are initialized according to today’s distribution [8], with most stake in Europe and North America. This lets us test whether protocol design amplifies or mitigates the centralization already present.

Evenly placed sources. We first simulate the setup where information sources are evenly positioned as in Section 4.2. Figure 5 shows that the system begins in a centralized state (high Gini and HHI), and both SSP and MSP continue to concentrate around the same low-latency hubs. The reason is straightforward: the incumbent hubs already enjoy propagation advantages that extend the viable window for timing games and boost payoffs, so marginal relocations mostly reinforce the status quo. While $c = 0.002$ appears to dampen further concentration, this is largely because the initial centralization leaves limited utility gains from additional moves; the direction of incentives remains unchanged.

Latency-aligned vs. mis-aligned sources. We now place the information sources unevenly as in Section 4.4, with a migration cost of $c = 0.002$. Results are shown in Figure 6. Under SSP, with high-latency relay placement, both Gini and HHI first decrease and then increase. This occurs because a relay in a poorly connected region (notably South America; see the top right panel in Figure 10) attracts validators to co-locate with it, causing many to migrate from regions

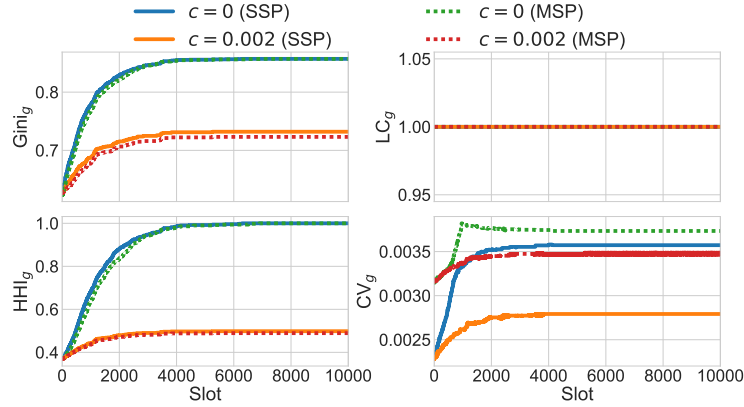


Fig. 5: *Setup: Heterogeneous validators with homogeneous information sources.* Evolution of centralization metrics under SSP and MSP with a heterogeneous validator distribution and homogeneous information sources.

with a high density of validators such as Europe and North America—briefly improving geographical decentralization. However, over time, the system converges toward every validator moving to this region, which worsens geographical decentralization again. With low-latency relay placement, since the vast majority of validators are already located in these regions, the marginal benefit of migration is small and centralization metrics stay consistent with Section 4.4.

Under MSP, unlike in Section 4.4, placing sources in high-latency regions does not slow down the pace of centralization. This stems from the fact that most validators are already clustered, so in the trade-off between latency to attesters and to sources, the outcome naturally favors the regions where validators are concentrated. As shown in Figure 10 (bottom right), North America and Europe retain their validator density. Further analysis of validator redistribution is provided in Section E.2.

Takeaway 4. With today’s already centralized validator geography, both SSP and MSP reinforce concentration around existing low-latency hubs when information sources are evenly placed. Introducing heterogeneous source placement changes this only marginally: in SSP, relays in poorly connected regions can briefly draw validators away from incumbent hubs, improving decentralization until full co-location occurs; in MSP, source placement has little effect, since proximity to attesters dominates incentives once validators are already clustered.

4.6 Further Experiments

Besides the above settings, we also use our simulation tool to assess geographical decentralization under different consensus configurations such as modified attestation thresholds or shorter slot times as in Ethereum Improvement Pro-

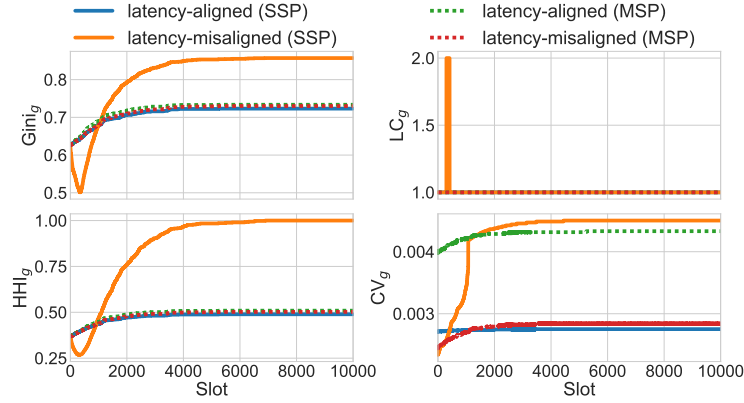


Fig. 6: *Setup: Heterogeneous validators and information sources.* Evolution of centralization metrics under SSP and MSP with latency-aligned vs. latency-misaligned source placement ($c = 0.002$).

posal (EIP)-7782 [1]. These results are presented in Section E.3 and Section E.4, respectively.

5 Discussion and Future Works

Latency data. In our simulations, latency and region information are based solely on GCP data. While this choice provides a consistent and publicly available dataset, it may introduce bias. Other cloud service providers may offer denser regional coverage and lower latency, which could affect validator connectivity and block propagation dynamics, and therefore could affect the simulation outcomes.

However, we note that other major cloud service providers, such as AWS, Azure, and OVH, exhibit broadly similar regional distributions [2,32,35]: most regions are in Europe, North America, and Asia. Moreover, since inter-regional latencies are largely determined by existing fiber-optic infrastructure, using data from alternative providers would likely yield comparable results. As future work, we plan to use datasets from other providers to further validate our findings.

Value function. In our simulations, the value function is modeled as a deterministic function, monotonically increasing over time. This choice allows us to simplify validator strategies and make them computationally tractable. Nevertheless, it abstracts away potential variability in practice, such as stochastic transaction arrivals or builder-specific behaviors, which we leave for future work. Under MSP, we further assume that signals from different sources are additive. In reality, overlapping signals would likely yield a sub-linear aggregate value. Finally, we treat information sources as fungible with identical value parameters, although in practice different relays or signals may provide heterogeneous value per unit time.

Migration. Our model assumes that migration occurs instantaneously and at a constant cost. This approximation is motivated by the fact that validators can anticipate their duties and pre-synchronize nodes in the destination region. In practice, migration may involve variable delays and costs, which we leave for future work on modeling more complex migration processes.

Block-building paradigms. We study two paradigms: SSP and MSP. Under MSP (local block-building), proposers aggregate value from multiple sources (e.g., mempools), construct the block and propagate it. This makes geography directly affect marginal value—shorter latencies both raise the payoff of waiting and widen the window for timing strategies—thereby strengthening incentives to migrate and form hubs in low-latency regions. By contrast, SSP-like designs (e.g., MEV-Boost) abstract information aggregation away from proposers via relays that supply and propagate blocks. When relay placement is well-distributed, SSP can homogenize marginal value across regions and dampen co-location incentives; conversely, poorly placed or sparse relays can become focal points for centralization. Our results indicate that without PBS, migration pressures to capture more MEV would be stronger, leaving non-migrating validators behind and intensifying centralization. By contrast, PBS enables more symmetric access to value—provided relays are strategically placed. As future work, we plan to study proposals such as Multiple Concurrent Proposers (MCP) [34], discussed as critical for Ethereum’s censorship resistance.

6 Related Work

Blockchain decentralization. Prior work has measured (de)centralization using diverse metrics. The Nakamoto coefficient was introduced to capture the minimum number of entities needed to compromise a blockchain subsystem [41]. Other measures, including the Gini coefficient [12], Shannon entropy [29], and the Herfindahl–Hirschman index [38], have been applied to quantify (de)centralization in various contexts, such as mining power [28,30,49], staking distribution [21,28], and block building [22,37,50]. Our work examines a different dimension by proposing metrics that capture the geographical distribution of validators.

Geographical location of Ethereum validators. Validators’ geo-location has received less attention despite its importance for latency and fault tolerance. Kim et al. developed NodeFinder to measure Ethereum Peer-to-Peer (P2P) networks during the Proof-of-Work (PoW) era, finding that as of 2018, most nodes were in the U.S. (43.2%), China (12.9%), and Germany (5.2%) [26]. Similar inference methods have been applied to the PoS era [5], showing continued concentration in a few countries. Online dashboards [13,7] report real-time Ethereum node distribution and, as of September 2025, identify the United States and Germany as dominant. Heimbach et al. further developed a deanonymization technique that located over 15% of validators, with more than 85% situated in Europe and North America [23].

ABM in blockchain. ABM has been widely adopted to model the strategic behavior of blockchain participants. Kraner et al. modeled Ethereum PoS

to analyze how network topology and latency influence consensus performance and stability [27]. Öz et al. examined the impact of waiting games on consensus stability, showing that delay strategies can be profitable without undermining consensus when widely adopted [36]. Other works used ABM to study builder behaviors in MEV-Boost auctions [47,48], assess design proposals such as Execution Tickets [42], and analyze how staking and inflation policies shape token concentration in DAO and DeFi governance [9].

7 Conclusion

In this paper, we investigated how protocol design, given existing network infrastructure, shapes the geographical decentralization of Ethereum by altering validator incentives. We introduced a latency-calibrated agent-based simulation framework that enables counterfactual analysis of validator migration under different structural and protocol settings. Our results show that protocol design strongly conditions validator incentives and thus geographic outcomes: validators slowly centralize around relay placement under SSP since proximity only affects block propagation, while MSP amplifies migration toward latency minima because block value aggregates from multiple regions. Heterogeneous source placement and consensus settings can either reduce or heighten these pressures, but positive effects on geographical decentralization are limited once validators are already clustered. Across almost all settings, North America remains the dominant destination due to its latency advantage. Overall, these insights can guide future protocol designs that better align incentives with geographical decentralization.

References

1. Adams, B., Feist, D.: EIP-7782: Reduce Block Latency [DRAFT]. Ethereum Improvement Proposals (7782) (October 2024), <https://eips.ethereum.org/EIPS/eip-7782>, [Online serial]
2. Amazon Web Services, Inc.: Aws global infrastructure. <https://aws.amazon.com/about-aws/global-infrastructure/> (2025), accessed: 2025-09-17
3. Authors: Geographical decentralization simulation. <https://geo-decentralization.github.io/> (2025)
4. Blockchain.com: Hashrate distribution (pools). <https://www.blockchain.com/explorer/charts/pools> (2025), accessed: 2025-09-09
5. Bostoen, J., Garg, N.: Estimating validator decentralization using p2p data. <https://ethresear.ch/t/estimating-validator-decentralization-using-p2p-data/19920> (June 27 2024)
6. Buterin, V., Hernandez, D., Kamphefner, T., Pham, K., Qiao, Z., Ryan, D., Sin, J., Wang, Y., Zhang, Y.X.: Combining ghost and casper. arXiv preprint arXiv:2003.03052 (2020)
7. Cambridge Centre for Alternative Finance (CCAF): Ethereum network analytics. https://ccaf.io/cbnsi/ethereum/network_analytics (2025), accessed September 1, 2025

8. Chainbound: Geolocating validators. <https://dune.com/chainbound/geolocating-validators> (2024), accessed: 2025-08-18
9. Cong, L.W., Dong, Y., Lu, Y., Ruan, Q., Wang, G.: Agent-based modeling for daos and defi. Available at SSRN 5171559 (2024)
10. Cong, L.W., He, Z., Li, J.: Decentralized mining in centralized pools. *The Review of Financial Studies* **34**(3), 1191–1235 (2021)
11. Daian, P., Goldfeder, S., Kell, T., Li, Y., Zhao, X., Bentov, I., Breidenbach, L., Juels, A.: Flash boys 2.0: Frontrunning in decentralized exchanges, miner extractable value, and consensus instability. In: 2020 IEEE symposium on security and privacy (SP). pp. 910–927. IEEE (2020)
12. Dorfman, R.: A Formula for the Gini Coefficient. *The review of economics and statistics* pp. 146–149 (1979)
13. ethernodes.org: Ethernodes – countries. <https://www.ethernodes.org/countries> (2025), accessed: 2025-09-01
14. Flashbots: Overview – mev-boost. <https://docs.flashbots.net/flashbots-mev-boost/introduction> (2025), accessed: 2025-08-03
15. Foundation, E.: Proposer-builder separation. <https://ethereum.org/en/roadmap/pbs/> (2024), accessed: 2025-08-13
16. Foundation, E.: Ethereum proof-of-stake consensus specifications. <https://github.com/ethereum/consensus-specs> (2025), accessed: 2025-09-09
17. Foundation, E.: The merge. <https://ethereum.org/en/roadmap/merge/> (2025)
18. Gencer, A.E., Basu, S., Eyal, I., Van Renesse, R., Sirer, E.G.: Decentralization in bitcoin and ethereum networks. In: *International conference on financial cryptography and data security*. pp. 439–457. Springer (2018)
19. Google: Google looker studio dashboard: fc733b10-9744-4a72-a502-92290f608571. <https://lookerstudio.google.com/reporting/fc733b10-9744-4a72-a502-92290f608571> (2025), accessed: 2025-09-11
20. Grandjean, D., Heimbach, L., Wattenhofer, R.: Ethereum proof-of-stake consensus layer: Participation and decentralization. In: *International Conference on Financial Cryptography and Data Security*. pp. 253–280. Springer (2024)
21. Grandjean, D., Heimbach, L., Wattenhofer, R.: Ethereum Proof-of-Stake Consensus Layer: Participation and Decentralization. In: *5th Workshop on Coordination of Decentralized Finance 2024* (2024)
22. Heimbach, L., Kiffer, L., Ferreira Torres, C., Wattenhofer, R.: Ethereum’s proposer-builder separation: Promises and realities. In: *2023 ACM Internet Measurement Conference (IMC), Montreal, QC, Canada* (2023)
23. Heimbach, L., Vonlanthen, Y., Villacis, J., Kiffer, L., Wattenhofer, R.: Deanonymizing ethereum validators: The p2p network has a privacy issue. In: *34th USENIX Security Symposium, Seattle, WA, USA* (2025)
24. ter Hoeven, E., Kwakkel, J., Hess, V., Pike, T., Wang, B., Kazil, J., et al.: Mesa 3: Agent-based modeling with python in 2025. *Journal of Open Source Software* **10**(107), 7668 (2025)
25. Hotelling, H.: Stability in competition. *The Economic Journal* **39**(153), 41–57 (1929). <https://doi.org/10.2307/2224214>
26. Kim, S.K., Ma, Z., Murali, S., Mason, J., Miller, A., Bailey, M.: Measuring ethereum network peers. In: *Proceedings of the Internet Measurement Conference 2018*. pp. 91–104 (2018)
27. Kraner, B., Vallarano, N., Schwarz-Schilling, C., Tessone, C.J.: Agent-based modelling of ethereum consensus. In: *2023 IEEE International Conference on Blockchain and Cryptocurrency (ICBC)*. pp. 1–8. IEEE (2023)

28. Kwon, Y., Liu, J., Kim, M., Song, D., Kim, Y.: Impossibility of Full Decentralization in Permissionless Blockchains. In: Proceedings of the 1st Conference on Advances in Financial Technologies (AFT). pp. 110–123 (2019)
29. Lin, J.: Divergence Measures Based on the Shannon Entropy. *IEEE Transactions on Information Theory* **37**(1), 145–151 (1991)
30. Lin, Q., Li, C., Zhao, X., Chen, X.: Measuring Decentralization in Bitcoin and Ethereum using Multiple Metrics and Granularities. In: 2021 IEEE 37th International Conference on Data Engineering Workshops (ICDEW). pp. 80–87. IEEE (2021)
31. Macal, C.M., North, M.J.: Tutorial on agent-based modeling and simulation. In: Proceedings of the Winter Simulation Conference, 2005. pp. 14–pp. IEEE (2005)
32. Microsoft Corporation: Azure regions list. <https://learn.microsoft.com/en-us/azure/reliability/regions-list> (2025), accessed: 2025-09-17
33. Nakamoto, S.: Bitcoin: A peer-to-peer electronic cash system. Available at SSRN 3440802 (2008)
34. Neuder, M., Resnick, M.: Concurrent Block Proposers in Ethereum. <https://ethresear.ch/t/concurrent-block-proposers-in-ethereum/18777> (2024)
35. OVHcloud: Ovhcloud locations: Global infrastructure locations. <https://us.ovhcloud.com/about/global-infrastructure/locations/> (2025), accessed: 2025-09-17
36. Öz, B., Kraner, B., Vallarano, N., Kruger, B.S., Matthes, F., Tessone, C.J.: Time moves faster when there is nothing you anticipate: The role of time in mev rewards. In: Proceedings of the 2023 Workshop on Decentralized Finance and Security. p. 1–8. DeFi '23, Association for Computing Machinery, New York, NY, USA (2023). <https://doi.org/10.1145/3605768.3623563>, <https://doi.org/10.1145/3605768.3623563>
37. Öz, B., Sui, D., Thiery, T., Matthes, F.: Who wins ethereum block building auctions and why? In: 6th Conference on Advances in Financial Technologies. p. 1 (2024)
38. Rhoades, S.A.: The Herfindahl–Hirschman Index. *Fed. Res. Bull.* **79**, 188 (1993)
39. Schwarz-Schilling, C., Saleh, F., Thiery, T., Pan, J., Shah, N., Monnot, B.: Time is money: Strategic timing games in proof-of-stake protocols. In: 5th Conference on Advances in Financial Technologies (2023)
40. Silva, M.I.: An analysis of attestation timings in a 6-s slot . <https://ethresear.ch/t/an-analysis-of-attestation-timings-in-a-6-s-slot/23016> (2025)
41. Srinivasan, B.S., Lee, L.: Quantifying Decentralization. *news.earn.com* (2017)
42. Stichler, P.: Galaxy era: Agent-based simulation of execution tickets. arXiv preprint arXiv:2501.16090 (2025)
43. Thorn, A., Fabiano, A., Helmy, K.: Examining the latest china bitcoin ban (May 2021), <https://www.galaxy.com/insights/research/examining-the-latest-china-bitcoin-ban>, research article
44. Wahrstätter, A., Ernstberger, J., Yaish, A., Zhou, L., Qin, K., Tsuchiya, T., Steinhorst, S., Svetinovic, D., Christin, N., Barczentewicz, M., et al.: Blockchain censorship. In: Proceedings of the ACM Web Conference 2024. pp. 1632–1643 (2024)
45. Wahrstätter, A., Zhou, L., Qin, K., Svetinovic, D., Gervais, A.: Time to bribe: Measuring block construction market. arXiv preprint arXiv:2305.16468 (2023)
46. Wu, F., Sui, D., Thiery, T., Pai, M.: Measuring cex-dex extracted value and searcher profitability: The darkest of the mev dark forest (2025), <https://arxiv.org/abs/2507.13023>
47. Wu, F., Thiery, T., Leonardos, S., Ventre, C.: Strategic bidding wars in on-chain auctions. In: 2024 IEEE International Conference on Blockchain and Cryptocurrency (ICBC). pp. 503–511. IEEE (2024)

48. Wu, F., Thiery, T., Leonardos, S., Ventre, C.: From competition to centralization: The oligopoly in ethereum block building auctions. In: 28th European Conference on Artificial Intelligence (ECAI) (2025)
49. Wu, K., Peng, B., Xie, H., Huang, Z.: An Information Entropy Method to Quantify the Degrees of Decentralization for Blockchain Systems. In: 2019 IEEE 9th International Conference on Electronics Information and Emergency Communication (ICEIEC). pp. 1–6. IEEE (2019)
50. Yang, S., Nayak, K., Zhang, F.: Decentralization of ethereum’s builder market. In: 2025 IEEE Symposium on Security and Privacy (SP). pp. 1512–1530. IEEE (2025)
51. Yang, S., Öz, B.: syang-ng/geographical-decentralization-simulation (Sep 2025), <https://github.com/syang-ng/geographical-decentralization-simulation>, original-date: 2025-06-09T13:40:22Z

A List of Google Cloud Platform Regions

In this section, we present the list of Google Cloud Platform (GCP) regions used in our paper, along with their physical locations, as shown in Table 2. We exclude two GCP regions—me-central2 (Dammam, Saudi Arabia) and northamerica-south1 (Queretaro, Mexico)—because latency data between these regions and the others was not available [19].

Figure 7 presents the heatmap of median latency between each pair of macro-regions. For example, the median latency between Asia and Europe is computed as the median value of all latencies between GCP regions in Asia and GCP regions in Europe. Among the seven macro-regions, North America has the best average median latency to other regions (142.97 ms), while South America has the worst (209.88 ms).

Table 2: GCP regions and their physical locations.

| Macro-Region | GCP Region | Location |
|---------------|-------------------------|------------------------------|
| Africa | africa-south1 | Johannesburg, South Africa |
| Asia | asia-east1 | Changhua County, Taiwan |
| | asia-east2 | Hong Kong, China |
| | asia-northeast1 | Tokyo, Japan |
| | asia-northeast2 | Osaka, Japan |
| | asia-northeast3 | Seoul, South Korea |
| | asia-south1 | Mumbai, India |
| | asia-south2 | Delhi, India |
| | asia-southeast1 | Singapore |
| Oceania | asia-southeast2 | Jakarta, Indonesia |
| | australia-southeast1 | Sydney, Australia |
| Europe | australia-southeast2 | Melbourne, Australia |
| | europa-central2 | Warsaw, Poland |
| | europa-north1 | Hamina, Finland |
| | europa-north2 | Stockholm, Sweden |
| | europa-southwest1 | Madrid, Spain |
| | europa-west1 | St. Ghislain, Belgium |
| | europa-west2 | London, UK |
| | europa-west3 | Frankfurt, Germany |
| | europa-west4 | Eemshaven, Netherlands |
| | europa-west6 | Zurich, Switzerland |
| | europa-west8 | Milan, Italy |
| | europa-west9 | Paris, France |
| europa-west10 | Berlin, Germany | |
| europa-west12 | Turin, Italy | |
| Middle East | me-central1 | Doha, Qatar |
| | me-west1 | Tel Aviv, Israel |
| South America | southamerica-east1 | Sao Paulo, Brazil |
| | southamerica-west1 | Santiago, Chile |
| North America | northamerica-northeast1 | Montreal, Canada |
| | northamerica-northeast2 | Toronto, Canada |
| | us-central1 | Council Bluffs, Iowa, USA |
| | us-east1 | Moncks Corner, SC, USA |
| | us-east4 | Ashburn, Virginia, USA |
| | us-east5 | Columbus, Ohio, USA |
| | us-south1 | Dallas, Texas, USA |
| | us-west1 | The Dalles, Oregon, USA |
| | us-west2 | Los Angeles, California, USA |
| | us-west3 | Salt Lake City, Utah, USA |
| us-west4 | Las Vegas, Nevada, USA | |

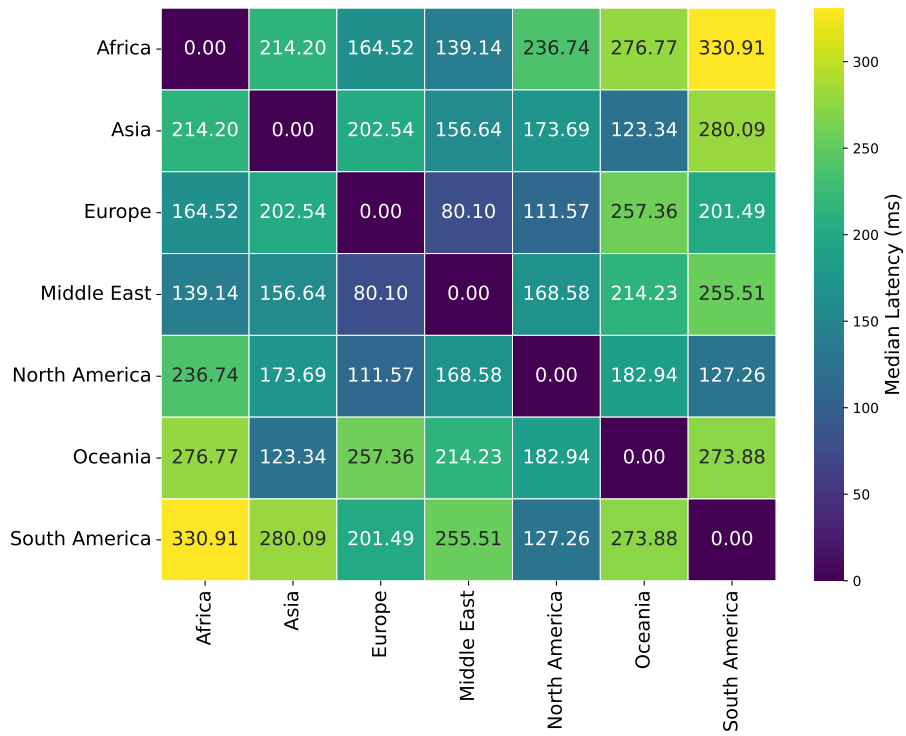


Fig. 7: Heatmap of median latency between macro-regions.

B List of Symbols

Table 3: List of symbols.

| Symbol | Description |
|-------------------------------------|------------------------------------------------------------------------|
| $\mathcal{R} = \{r_1, \dots, r_m\}$ | Set of regions |
| $\mathcal{V} = \{v_1, \dots, v_P\}$ | Set of validators (agents) |
| $d(r_j, r_k)$ | Latency between r_j to r_k (drawn from log-normal distribution) |
| μ_{jk} | Expected latency between r_j and r_k |
| c | Cost of migration across regions |
| n | Slot index ($n \in \{1, \dots, N\}$) |
| p_n | Proposer of slot n |
| $r(p_n)$ | Region of the proposer of slot n |
| $a \in \mathcal{A}_n$ | An attester in the set of attesters assigned for slot n |
| $r(a)$ | Region of attester a |
| γ | Fraction of attesters required for canonicalization |
| Δ | Slot duration |
| τ | Block release time within slot |
| τ_{cut} | Cutoff time for attestations |
| R | Proposer's risk tolerance |
| \mathcal{I} | Set of information sources |
| $\mathcal{I}_{\text{signal}}$ | Set of signal sources |
| $\mathcal{I}_{\text{relay}}$ | Set of relay sources |
| $r(I)$ | Region of source I |
| $V_I(t) = a_I t + b_I$ | Value available from source I at time t |
| $V_r(\tau)$ | Aggregate block value at region r and release time τ |
| $q_a(\tau; r)$ | Probability that attester a votes on time if released at (r, τ) |
| $S(\tau; r)$ | Number of timely attestations if released at (r, τ) |
| $\Pi_r(\tau)$ | Probability block becomes canonical if released at (r, τ) |
| τ_r^* | Optimal release time in region r |
| $W(r)$ | Expected payoff in region r |
| τ_I^* | Optimal release time when using relay I |
| $W(I)$ | Expected payoff when using relay I |
| \mathcal{W} | The set of expected payoffs for a region $r \in \mathcal{R}$ |

C Geographical Decentralization Metric Definitions

In this section, we provide formal definitions of the metrics we used in our simulation.

Setup. Let \mathcal{R} denote the set of regions. For each $r \in \mathcal{R}$, let s_r be the total effective balance of validators located in r , and let $S = \sum_{r \in \mathcal{R}} s_r$. Define normalized shares

$$p_r = \frac{s_r}{S}, \quad p_r \geq 0, \quad \sum_{r \in \mathcal{R}} p_r = 1.$$

Geographical Gini. The geographical Gini coefficient is

$$\text{Gini}_g = \frac{1}{2|\mathcal{R}|} \sum_{r \in \mathcal{R}} \sum_{r' \in \mathcal{R}} |p_r - p_{r'}|.$$

It equals 0 under perfectly even stake distribution and increases with inequality (approaching $1 - 1/|\mathcal{R}|$ in the extreme of all stake in one region).

Geographical HHI. The geographical HHI is

$$\text{HHI}_g = \sum_{r \in \mathcal{R}} p_r^2,$$

with $\text{HHI}_g \in [1/|\mathcal{R}|, 1]$. Lower values indicate greater dispersion.

Geographical Payoff Coefficient of Variation (CV). Let \mathcal{W} denote the set of best payoffs for the proposer in region $r \in \mathcal{R}$ in one slot, the geographical payoff coefficient of variation is

$$\text{CV}_g = \frac{\sigma(\mathcal{W})}{\mu(\mathcal{W})},$$

where $\mu(\mathcal{W})$ and $\sigma(\mathcal{W})$ are the mean and standard deviation of \mathcal{W} , respectively. It grows as inter-regional disparities increase.

Liveness coefficient. To capture robustness against geographically correlated failures (e.g., natural disasters or country-level regulation), we adapt the Nakamoto coefficient to Ethereum PoS liveness. Ethereum PoS maintains liveness as long as at least 2/3 of the effective stake is online. Sort regions by stake share p_r in non-increasing order and let r_1, r_2, \dots denote that ordering. The *liveness coefficient* (LC_g) is the minimal k such that

$$\sum_{i=1}^k p_{r_i} \geq \frac{1}{3}.$$

Intuitively, it is the smallest number of (largest) regions whose simultaneous outage suffices to threaten liveness. Larger values indicate greater resilience.

D Marginal Benefit Distribution

Figure 8 shows the CDF of marginal benefits when proposers move to the best region during the first 1,000 slots of the baseline. Under SSP, about 80% of migration marginal benefits are less than 0.002, which suggests that such migration could be prevented if the migration cost is 0.002.

E Further Experiments

E.1 Migration Costs

We evaluate how migration costs affect both the degree and speed of geographical centralization. Using the homogeneous setup in Section 4.2, we vary the cost

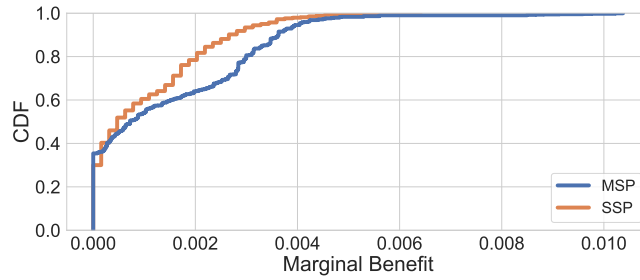


Fig. 8: CDF of marginal benefit in the first 1,000 slots of the baseline.

from 0 to 0.003; at the upper end of this range, the cost eliminates over 70% of the typical marginal relocation gain in both SSP and MSP (see Figure 8). As shown in Figure 9, higher costs predictably dampen validator mobility and mitigate centralization. The effect is consistently stronger under SSP than MSP, reflecting the mechanism in Section 4.2, Takeaway 1: in MSP, location directly shifts marginal value via multi-source aggregation, sustaining stronger incentives to co-locate even when migration is costly.

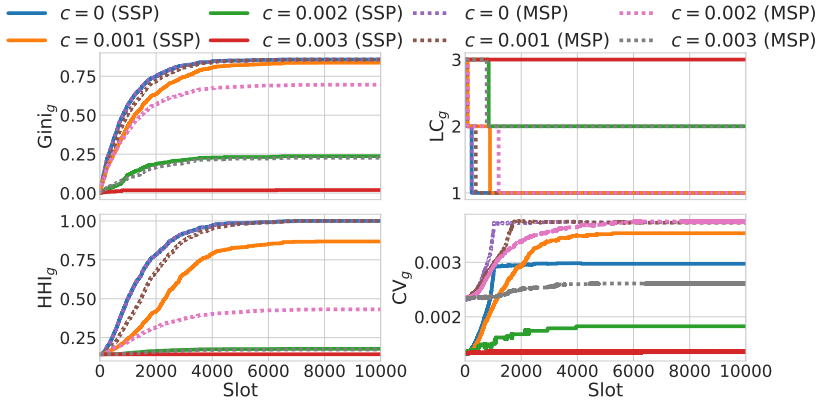


Fig. 9: *Setup: Homogeneous validators and information sources.* Evolution of centralization metrics under SSP and MSP with varying migration costs $c \in \{0, 0.001, 0.002, 0.003\}$.

E.2 Clustering in Real-World Validator Distribution

Figure 10 shows where centralization emerges when validators are initialized using today’s distribution [8], as in the experiments of Section 4.5.

In SSP, under the latency-misaligned case (upper-right panel), validators converge to South America. Since the majority of validators are initially located in North America and Europe, co-locating with a relay in South America provides a stronger latency advantage than co-locating with a relay in Africa or Oceania. For MSP, by contrast, a small fraction of validators migrate to North America in both the latency-aligned and latency-misaligned cases. Since the existing concentration of validators in North America and Europe creates a latency advantage to attesters, even when information sources are located elsewhere the trade-off still favors these regions.

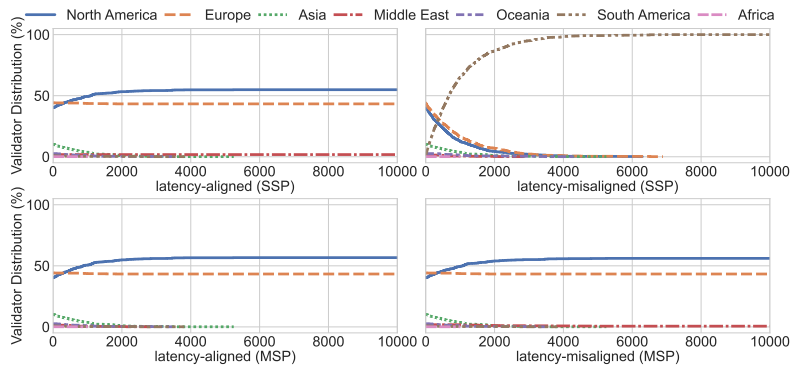


Fig. 10: *Setup: Heterogeneous validators and information sources.* Validator distribution aggregated by macro-regions under SSP and MSP in the latency-aligned case and latency-misaligned case.

E.3 Attestation Threshold

We now study how the required attestation threshold γ (the quorum needed for a block to become canonical) shapes geographical centralization. Specifically, we set γ to different values ($\frac{1}{3}$, $\frac{1}{2}$, $\frac{4}{5}$) and run the homogeneous baseline of Section 4.2 under both SSP and MSP.

Intuitively, a larger γ tightens the effective timing window, increasing the value of low-latency placement and thus strengthening co-location incentives. Figure 11 confirms this intuition for SSP: when $\gamma \leq \frac{1}{2}$, validators rarely migrate at cost $c = 0.002$, as reflected in both Gini and HHI indices. The variance in best attainable payoffs across regions also remains small, as shown in the bottom-right panel. Under MSP, by contrast, centralization pressure decreases with higher γ . The reason is that proposers face a sharper trade-off: they must remain close enough to attesters to satisfy the quorum, but also close to multiple information sources to maximize aggregate value. At lower thresholds, fewer attesters need to be reached, so validators are less constrained in prioritizing signals. Higher

thresholds force them to balance both dimensions, which reduces the relative benefit of migrating toward a single hub.

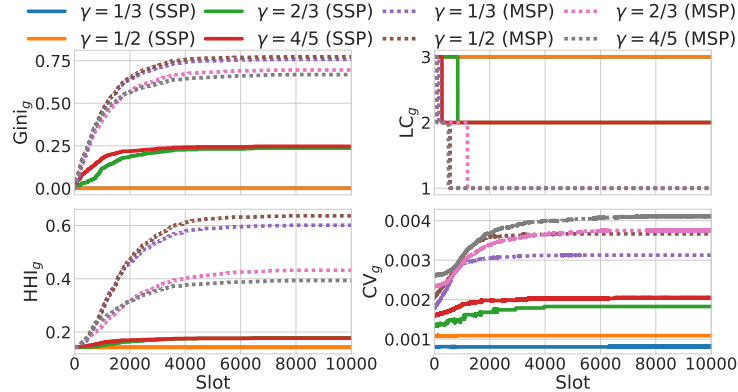


Fig. 11: *Setup: Homogeneous validators and information sources.* Evolution of centralization metrics under SSP and MSP with different attestation threshold ($\gamma \in \{\frac{1}{3}, \frac{1}{2}, \frac{2}{3}, \frac{4}{5}\}$) when $c = 0.002$. Note that the orange solid line largely overlaps with the blue solid line.

E.4 Shorter Slot Time

Reducing Ethereum’s slot time has been recently discussed in the community through EIP-7782 [1], which proposes $\Delta = 6$ s with an attestation deadline of $\tau_{\text{cut}} = 3$ s. The stated goals are higher throughput and better UX. Recent measurements [40] report sub-second pure block propagation, suggesting feasibility.

We simulate EIP-7782 under both SSP and MSP using the homogeneous baseline of Section 4.2 to assess its impact on geographical decentralization relative to today’s parameters ($\Delta = 12$ s, $\tau_{\text{cut}} = 4$ s). Because observed propagation delays are small relative to the shortened windows, proposers face essentially the same co-location trade-offs as at $\Delta = 12$ s. Consequently, the Gini and HHI trajectories are nearly unchanged in both paradigms (see Figure 12), aligning with [40].

However, we do observe a higher payoff coefficient of variation (CV_g) across regions for $\Delta = 6$ s in both SSP and MSP (although the increase appears less pronounced for SSP in Figure 12), indicating that shorter slots amplify reward dispersion even if they do not materially alter the centralization trend. This arises because the latency advantage is close to an absolute value: when the slot is only 6, s, the same latency edge translates into a larger share of the timing window, making the marginal benefit of advantage higher and cross-region variance more pronounced.

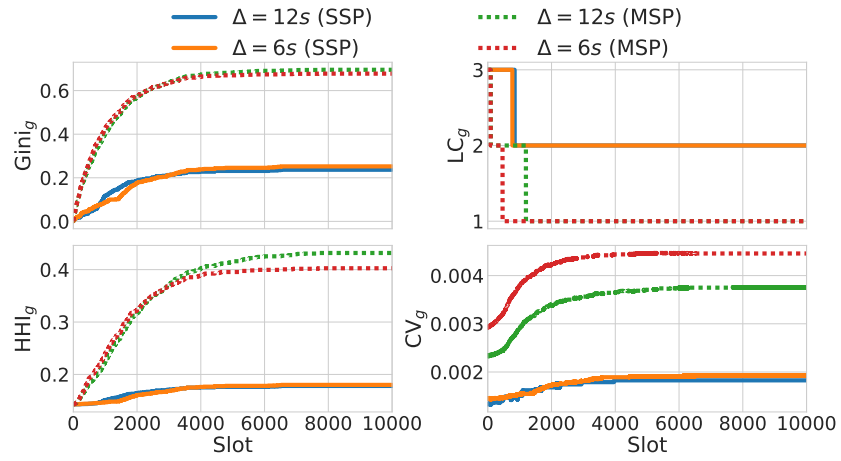


Fig. 12: *Setup: Homogeneous validators and information sources.* Evolution of centralization metrics under SSP and MSP with shorter ($\Delta = 6$ s) versus current slot times ($\Delta = 12$ s) when $c = 0.002$.